

# INTEGRAL YIELDS OF PHOTONEUTRON REACTIONS ON TIN ISOTOPES $^{118}\text{Sn}$ AND $^{124}\text{Sn}$ IN THE NEAR-THRESHOLD ENERGY REGION

Ye. Skakun<sup>1</sup>, I. Semisalov<sup>1</sup>, A. Chekhovska<sup>1</sup>, S. Karpus<sup>1,2</sup>

<sup>1</sup>National Science Center “Kharkiv Institute of Physics and Technology”, Kharkiv, Ukraine;

<sup>2</sup>Lutsk National Technical University, Lutsk, Ukraine

E-mail: semisalovigore@gmail.com

The integral yields of the photonuclear reactions  $^{118}\text{Sn}(\gamma, n)^{117\text{m}}\text{Sn}$  and  $^{124}\text{Sn}(\gamma, n)^{123\text{m}}\text{Sn}$ , which are of interest for studying scenarios of the formation of atomic nuclei in stars, are measured in the near-threshold energy region. The experimental data are compared with the results of theoretical calculations performed using the TALYS nuclear reaction code. The dependence of theoretical predictions on the choice of models of the nuclear level density and the radiative strength function is investigated.

PACS: 25.20.-x, 27.60.+q

## INTRODUCTION

Studies of photon-induced nuclear reactions is important for understanding the structure of the nucleus and nuclear interactions, i.e. for fundamental nuclear physics, and experimental data on photon reactions have a wide range of practical applications and contribute to the development of related sciences. In particular, integral yields and/or cross sections of photonuclear reactions are needed to model nucleosynthesis scenarios in the Universe.

Photonuclear reactions play a crucial role in the stellar nucleosynthesis of the so-called *p-nuclei* [1] – 35 naturally observed stable proton-rich nuclei, which, due to the peculiarities of some isobaric chains in the periodic table, could not be formed in slow or fast neutron capture reactions (*s*- and *r*-processes) [2, 3], which had produced the vast majority of medium and heavy atomic nuclei.

The main motivation for the development of the theory of cosmic nucleosynthesis is the understanding of the shape of the stable isotope abundance curve plotted as a function of atomic mass and the significant difference (up to ten million times) in the abundance of different chemical elements and some their isotopes.

*p*-Nuclei represent only a small part (usually 0.01...1%) of the isotopic content of the corresponding elements in the Solar System. This fact gives us hope to believe in the scenario of *p*-nuclei production from pre-existing *s*- and *r*-nuclei. Since (*p*, $\gamma$ )-reactions, which can also produce *p*-nuclei, require too high a stellar plasma temperature to overcome the proton Coulomb barrier, photonuclear reactions may play a key role in the synthesis of *p*-nuclei, located in the mass range from selenium (Se) to mercury (Hg), and therefore the sub-scenario of *p*-nuclei formation by complex sequences of ( $\gamma, n$ ), ( $\gamma, p$ ), and ( $\gamma, \alpha$ )-reactions was called the  *$\gamma$ -process*. The most suitable astrophysical site for the  *$\gamma$ -process* is the deep oxygen-enriched neon layers of massive stars exploding as type II supernovae [4–6] at stellar plasma temperatures  $T_9=1.8...3.3$  ( $T_9$  is the temperature in units of  $10^9$  degrees Kelvin).

The available astrophysical nucleosynthesis modelling codes are likely to have their own

uncertainties, but they must be supplied with highly accurate nuclear data such as 1) reaction rates obtained from cross sections; 2) nuclear masses; 3) radionuclide decay data; 4) structural features of many nuclei, etc. The  *$\gamma$ -process* involves thousands of photonuclear reactions on about 2000 target nuclei, many of which are radioactive even in the ground state and often in excited states according to the Boltzmann statistics of stellar gas at high temperatures.

The chemical element tin (Sn) has the largest number of stable isotopes with masses between 112 and 124 atomic masses among which there are 3 *p*-nuclei ( $^{112}\text{Sn}$ ,  $^{114}\text{Sn}$ , and  $^{115}\text{Sn}$ ). In our previous studies, using the bremsstrahlung photon beam of the LUE-300 linear electron accelerator, we determined the experimental integral yields of the  $^{112}\text{Sn}(\gamma, n)^{111}\text{Sn}$  and  $^{114}\text{Sn}(\gamma, n)^{113}\text{Sn}$  photonuclear reactions in the near-threshold energy region, which will be useful for further analysis of the production of  $^{112}\text{Sn}$  and  $^{114}\text{Sn}$  *p*-nuclei in stars.

The need to have, but the impossibility of measuring, nuclear reaction cross sections on unstable and excited nuclei under terrestrial conditions increases the importance of theoretical calculations of nuclear reaction cross sections adapting the Hauser-Feshbach statistical model [7]. Therefore, the experimental values of nuclear reaction cross sections at low energies are the nuclear data for stellar nucleosynthesis modelling, and on the other hand, they are used to test the predictive power of the statistical theory of nuclear reactions.

In the present work, we report the results of measurements of the integral yields of photonuclear reactions of  $^{118}\text{Sn}(\gamma, n)^{117\text{m}}\text{Sn}$  and  $^{124}\text{Sn}(\gamma, n)^{123\text{m}}\text{Sn}$  with the production of isomeric states of final nuclei in the region of incident energies of  $\gamma$ -quanta important for the study of stellar nucleosynthesis, and calculations of cross sections of these reactions within the framework of statistical theory.

## EXPERIMENT

The photoactivation measurement technique was used in the experimental studies. The targets were irradiated by the bremsstrahlung photon flux of the linear electron accelerator of the NSC KIPT (Kharkiv). The energy of the accelerated electrons was determined

using a calibrated deflection sectional electromagnet and ranged from 9 to 14 MeV in our experiments. The energy distribution of the electron beam was 2...3%. At the accelerator output, the turned electron beam passed through a 50  $\mu\text{m}$  titanium foil and interacted with a 100  $\mu\text{m}$  tantalum converter. As a result, a bremsstrahlung photon flux was generated, which hit irradiated targets located at a distance of 40 cm from the converter along the beam axis. The electron beam was deflected from the axis by a powerful constant magnet. The stability and intensity of the photon flux during the irradiation of the targets were controlled by an ionisation chamber installed along the photon beam. To protect from background radiation, the ionisation chamber was installed in a lead casing. The average current of the electron beam was 15...20  $\mu\text{A}$ .

The tin targets were free foils of 10 $\times$ 10 mm and 20 mg in weight, which were produced by

electrodeposition of the desired material. Simultaneously with the tin targets, gold targets ( $^{197}\text{Au}$  monoisotope) were irradiated. These were discs with a diameter of 20 mm, each of which had a precisely measured weight of about 120 mg. We used the  $^{197}\text{Au}$  ( $\gamma, n$ ) $^{196}\text{Au}$  reaction as a standard for determining the photon flux intensity. The integral yields of the product nuclei were measured with a high-resolution Canberra HPGe gamma-ray spectrometer.

## EXPERIMENTAL RESULTS

Fig. 1 shows the energy diagrams of photoneutron reactions on  $^{118}\text{Sn}$  and  $^{124}\text{Sn}$  target nuclei and decays of radioactive product nuclei  $^{117\text{m}}\text{Sn}$  and  $^{123\text{m}}\text{Sn}$ , and the numerical data of the reaction thresholds, half-lives, energies, and branching factors of the observed gamma transitions are given in Table.

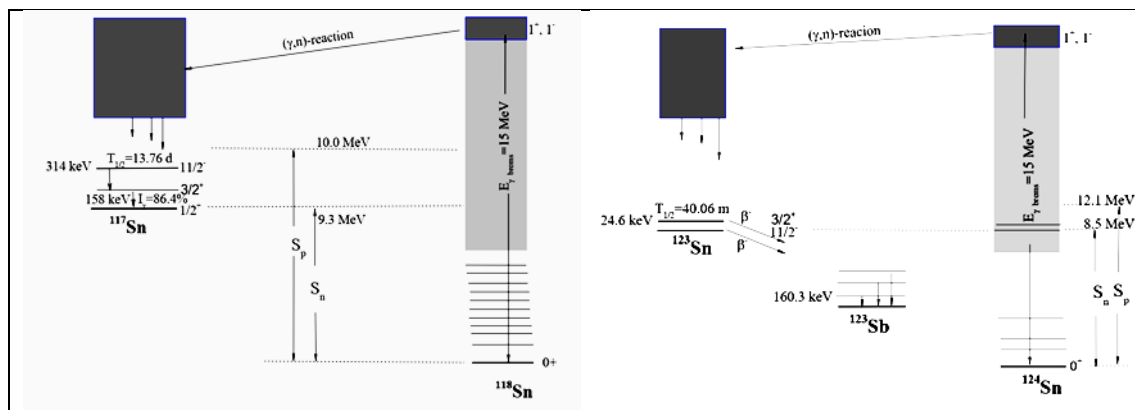


Fig. 1. Energy diagrams of photoneutron reactions on target nuclei  $^{118}\text{Sn}$  and  $^{124}\text{Sn}$  and simplified decay diagrams of isomeric  $^{117\text{m}}\text{Sn}$  and  $^{123\text{m}}\text{Sn}$  nuclei

To determine the yields of the  $^{118}\text{Sn}(\gamma, n)^{117\text{m}}\text{Sn}$  and  $^{124}\text{Sn}(\gamma, n)^{123\text{m}}\text{Sn}$  reactions, the experimentally measured intensities of strong radiative transitions with energies

of 158 and 160 keV were used, respectively. Nuclear data for the monitor  $^{197}\text{Au}(\gamma, n)^{196}\text{Au}$  reaction are also given in the last lines of the Table.

Reaction thresholds and spectroscopic data of the product nuclei [8]

Reaction	Reaction threshold, MeV	Product nuclei, Isomer spin	Half-lives	$E_\gamma$ , keV	Branching factor, %
$^{118}\text{Sn}(\gamma, n)$	9.642	$^{117\text{m}}\text{Sn}$ , $J^\pi=11/2^-$	13.60 d	156.02 158.56	2.113 86.4
$^{124}\text{Sn}(\gamma, n)$	8.513	$^{123\text{m}}\text{Sn}$ , $J^\pi=3/2^+$	40.06 m	160.33	85.69
$^{197}\text{Au}(\gamma, n)$	8.072	$^{196}\text{Au}$	6.17 d	333.03 355.73 426.10	22.87 86.95 6.59

## CALCULATIONS OF THE EXPERIMENTAL ACTIVATION YIELDS

The experimental integral activation yield  $Y_{\text{act}}(E_0)$  of ( $\gamma, n$ )-reaction, normalised per target nucleus and per unit of bremsstrahlung radiation with final energy  $E_0$ , is determined by the traditional activation equation from the intensity  $N_\gamma$  of the corresponding  $\gamma$ -line

$$Y_{\text{act}}(E_0) = \frac{N_\gamma}{N_t \varepsilon B} \exp(\lambda t_1) / \left\{ \frac{[1 - \exp(-\lambda t_2)]}{\lambda} \times [1 - \exp(-\lambda t_3)] \right\}, \quad (1)$$

where  $N_t$  is the number a of target nuclei;  $\lambda$  is the radioactive decay constant;  $\varepsilon$  is the detector efficiency;

$B$  is the branching factor of the observed  $\gamma$ -transition;  $t_1$ ,  $t_2$ , and  $t_3$  are the irradiation, cooling and activity measurement times of the sample, respectively.

To estimate the ( $\gamma, n$ )-reaction cross sections, we used the Lorentz function in the energy range from the ( $\gamma, n$ )-reaction threshold to the ( $\gamma, 2n$ )-reaction one:

$$\sigma(E) = \sigma_0 \left( \frac{E - S_n}{S_n} \right)^p \frac{1}{1 + \frac{(E^2 - E_R^2)^2}{E^2 \Gamma^2}}, \quad (2)$$

in which  $\sigma_0$ ,  $p$ ,  $E_R$ , and  $\Gamma$  values are fitted by the least-squares method to the giant resonance parameters.

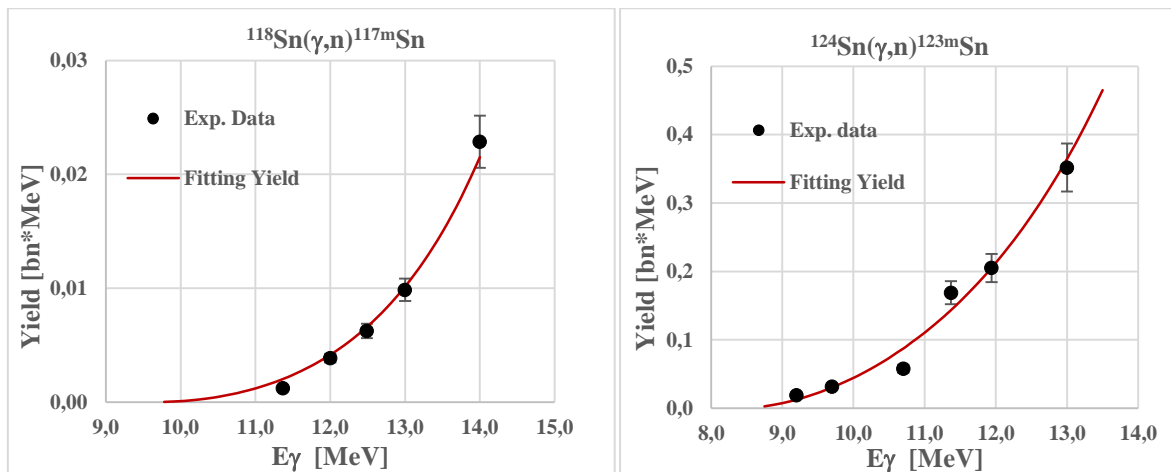


Fig. 2. Experimental (points) and fitted by equation (2) (curves) the integral yields of the  $^{118}\text{Sn}(\gamma,n)^{117m}\text{Sn}$  and  $^{124}\text{Sn}(\gamma,n)^{123m}\text{Sn}$  reactions

In Fig. 2, the dots show our experimental values of the integral yields of the photonuclear reactions of  $^{118}\text{Sn}(\gamma,n)^{117m}\text{Sn}$  (left graph) and  $^{124}\text{Sn}(\gamma,n)^{123m}\text{Sn}$  (right graph). The curves are the result of fitting equation (2) to the experimental data. The values of the parameters  $\sigma_0$ ,  $p$ ,  $E_R$ , and  $\Gamma$  obtained by the fitting procedure are 25.18 mbn, 0.402, 15.50, and 4.08 MeV, and 245.0 mbn, 0.07, 15.91, and 5.91 MeV for the reactions  $^{118}\text{Sn}(\gamma,n)^{117m}\text{Sn}$  and  $^{124}\text{Sn}(\gamma,n)^{123m}\text{Sn}$ , respectively.

### PRELIMINARY LITERATURE DATA AND THEORETICAL PREDICTIONS OF THE CROSS SECTIONS OF THE STUDIED REACTIONS

Previously, the experimental integral yields or cross sections of the  $^{118}\text{Sn}(\gamma,n)^{117}\text{Sn}$  and  $^{124}\text{Sn}(\gamma,n)^{123}\text{Sn}$  photon reactions were determined by the neutron registration technique. Varlamov et al. [9] analysed and evaluated the experimental cross sections of photonuclear reactions on tin isotope nuclei determined in different laboratories in the twentieth century, and the Utsunomiya group [10] performed new measurements after 2000. These data represent the total cross sections of the reactions, in contrast to the cross sections of the production of isomeric states that we have measured for the first time.

Fig. 3 shows the excitation function for the total production of a  $^{117}\text{Sn}$  nucleus in the  $^{118}\text{Sn}(\gamma,n)^{117\text{Tot}}\text{Sn}$  photonuclear reaction in the near-threshold energy range measured by Utsunomiya and co-workers [10] (green curve with dots) and estimated by Varlamov's group [9] from previous literature data obtained by other authors (blue curve with dots). In addition to the experimental data, the figure shows the predictions of the statistical theory (solid red and blue dashed curves).

We calculated the theoretical dependences of the reaction cross section using the well-known computer code TALYS [11, 12]. This code is the programmed Hauser-Feshbach statistical theory [7], the main ingredients of which are the optical model potential, the level density (**ld**) of excited nucleus, and the radiation strength function (**st**).

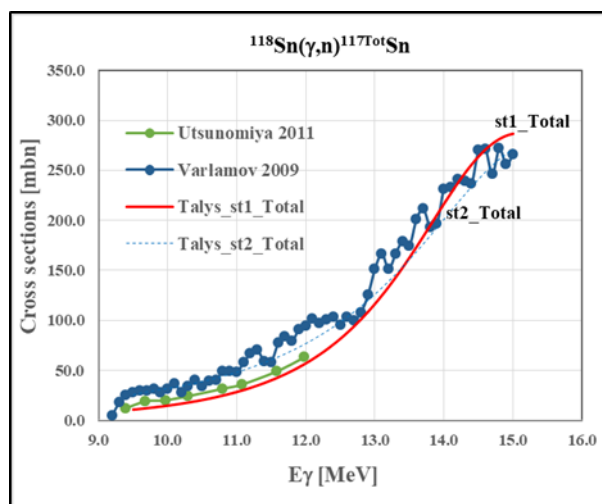


Fig. 3. Excitation function for total production of  $^{117}\text{Sn}$  nucleus in the  $^{118}\text{Sn}(\gamma,n)^{117\text{Tot}}\text{Sn}$  photonuclear reaction

TALYS code offers several models of the level density (**ld**) of the nucleus and several models of E1 gamma-radiation strength function (**st**).

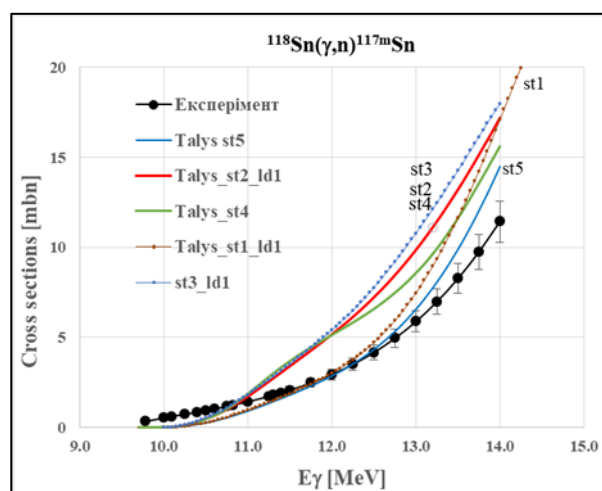


Fig. 4. Experimental (black dots) and theoretical (coloured curves) excitation functions of the  $^{118}\text{Sn}(\gamma,n)^{117m}\text{Sn}$  photonuclear reaction producing  $^{117}\text{Sn}$  nucleus in the metastable state

Fig. 4 illustrates the energy dependence of the cross-section of the  $^{118}\text{Sn}(\gamma,n)^{117\text{m}}\text{Sn}$  reaction to form a  $^{117}\text{Sn}$  nucleus in the isomeric state. The black dots represent the data obtained from our experimental data on the reaction yields by the least squares method (see Fig. 2), and the coloured curves show the theoretical values of the reaction cross sections in five radiation strength (st) function models. The closest to the experiment are the Brink-Axel Lorentzian model (st1) and the hybrid Goriely model (st5), although the steepness of the experimental and theoretical curves at different energy regions of the incident photons is different.

Similar data for the  $^{124}\text{Sn}(\gamma,n)^{123\text{m}}\text{Sn}$  reaction are shown in Fig. 5. The model (st2) of the generalised Kopetsky-Uhl lorentzian shows good agreement with the experiment. It is noteworthy that the contribution of the isomeric state formation cross section to the total cross section of the  $^{124}\text{Sn}(\gamma,n)^{123\text{m}}\text{Sn}$  reaction is much larger, which may be due to the low angular momentum of the  $^{123\text{m}}\text{Sn}$  nucleus compared to the  $^{117\text{m}}\text{Sn}$  nucleus. In this regard, further studies of the models of the nuclei level sincerity will be useful.

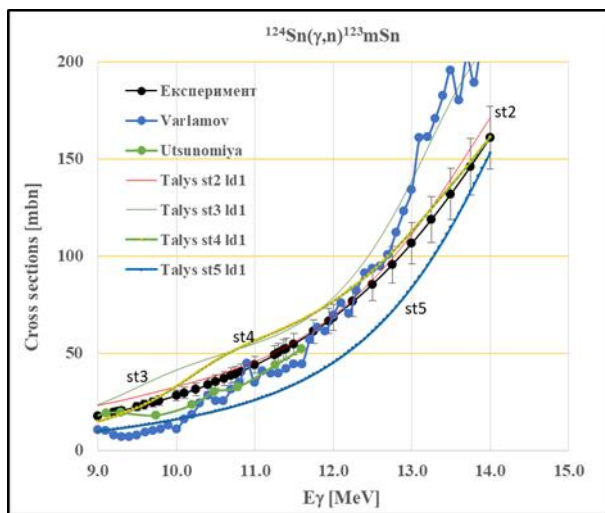


Fig. 5. Experimental (black dots) and theoretical (coloured curves) excitation functions of the  $^{124}\text{Sn}(\gamma,n)^{123\text{m}}\text{Sn}$  photonuclear reaction producing  $^{123}\text{Sn}$  nucleus in the metastable state

## CONCLUSIONS

Experimental measurements of integral yields and cross sections of photonuclear reactions in the low-energy region seem to be important for the study of stellar nucleosynthesis processes. To study p-nuclei production scenarios alone, experimental data for more than 10,000 reactions on ~2000 target nuclei are

required. At present, this data network is far from complete. The activation methodology, unlike the neutron registration methodology in the  $(\gamma,n)$ -reaction, observes a specific target nucleus, which excludes the influence of reactions on the nuclei of the accompanying isotopes always present in any target. The experimental results on the cross sections of the formation of isomeric states of the final nuclei provide an additional opportunity to test the statistical theory of nuclear reactions.

## REFERENCES

1. T. Rauscher. Origin of the p-nuclei in explosive nucleosynthesis // *Nuclei in the Cosmos XI*, Heidelberg / Ed. by K. Blaum, N. Christlieb, G. Martinez-Pinedo, 2010, Proceedings of Science, PoS(NIC XI) 059.
2. E.M. Burbidge, G.R. Burbidge, W.A. Fowler, and F. Hoyle. Synthesis of the elements in stars // *Rev. Mod. Phys.* 1957, v. 29, p. 547-650.
3. A.G.W. Cameron. Nuclear reactions in stars and nucleogenesis // *Publications of the Astronomical Society of the Pacific*. 1957, v. 69, p. 201-222.
4. M. Arnold, S. Goriely. The p-process of stellar nucleosynthesis: astrophysics and nuclear physics status // *Phys. Rep.* 2003, v. 384, p. 1-84.
5. W. Rapp, J. Gorres, M. Wiescher, H. Schatz, F. Kappeler. Sensitivity of p-process nucleosynthesis to nuclear reaction rates in a 25 M supernova model // *Astrophys. J.* 2006, v. 653, p. 474-489.
6. T. Rauscher. Branchings in the  $\gamma$ -process path revisited // *Phys. Rev.* 2006, v. C73, p. 015804.
7. W. Hauser and H. Feshbach. The inelastic scattering of neutrons // *Phys. Rev.* 1952, v. 87, p. 366-373.
8. <http://www.nndc.bnl.gov/nudat3/>
9. V.V. Varlamov, B.S. Ishkhanov, V.N. Orlin, V.A. Tchertvertkova // *Journ.: Izv. Rossiiskoi Akademii Nauk, Ser. Fiz.* 2010, v. 74, p. 875 (in Russian).
10. H. Utsunomiya et al. // *Phys. Rev.* 2011, C84, 055805. A. Koning, S. Hilaire, and M. Duijvestijn, in *Nuclear Data for Science and Technology*, edited by O. Bersillon, F. Gunsing, E. Bauge, R. Jacqmin, and S. Leray (EDP Sciences, Les Ulis, France, 2008), p. 211.
11. A. Koning and D. Rochman // *Nucl. Data Sheets.* 2012, v. 113, p. 2841.
12. E. Alhassan, D. Rochman, A. Vasiliev, A.J. Koning, H. Ferroukhi. TENDL-based evaluation and adjustment of p+ $^{111}\text{Cd}$  between 1 and 100 MeV // *Applied Radiation and Isotopes.* 2023, v. 198, p. 110832.

Article received 25.09.2024

## ІНТЕГРАЛЬНІ ВИХОДИ ФОТОЯДЕРНИХ РЕАКЦІЙ НА ІЗОТОПАХ ОЛОВА $^{118}\text{Sn}$ ТА $^{124}\text{Sn}$ У ПРИПОРОГОВІЙ ОБЛАСТІ ЕНЕРГІЙ

Є. Скакун, І. Семісалов, А. Чеховська, С. Карпуть

Інтегральні виходи фотоядерних реакцій  $^{118}\text{Sn}(\gamma,n)^{117\text{m}}\text{Sn}$  та  $^{124}\text{Sn}(\gamma,n)^{123\text{m}}\text{Sn}$ , які становлять інтерес для вивчення сценаріїв утворення атомних ядер у зірках, виміряно в енергетичному діапазоні енергій 9...14 MeV кінцевої точки гальмівного випромінювання лінійного пришвиджувача електронів та розраховано з використанням комп'ютерного коду TALYS. Досліджується залежність теоретичних передбачень від варіації моделей щільності ядерних рівнів ядра та фотонної силової функції.